JOURNAL OF
Materials
CHEMISTRY

The crystal chemistry of amide-functionalized ethylenedithiotetrathiafulvalenes: EDT-TTF-CONRR′ (R, R′ = H, Me)

Karine Heuzé, Marc Fourmigué* and Patrick Batail*

Institut des Matériaux Jean Rouxel, 2, rue de la Houssinière, BP32229, 44322 Nantes cedex 3, France

Received 12th April 1999, Accepted 21st July 1999

The preparation of ethylenedithiotetrathiafulvalenes (EDT-TTF) directly functionalized on the TTF core with a primary, secondary or tertiary amide or an hydrazide functional group is described. The X-ray crystal structures of EDT-TTF-CO_2H, EDT-TTF-$CONH_2$, EDT-TTF-CONHMe and EDT-TTF-$CONMe_2$ are reported. The solid state architectures adopted by those functionalized molecules appear to be a compromise between the hydrogen bond requirements of the OH, NH_2, CH and C=O groups, which act as hydrogen bond donor and acceptor, respectively, and the S···S van der Waals interactions of the EDT-TTF moiety. The activation of the hydrogen atom of the TTF core, *ortho* to the amidic group, enhances its involvement in short C–H···O bonds, giving rise to a characteristic chelating R_2^1 (7) motif as observed in the secondary amide, EDT-TTF-CONHMe.

Introduction

The occurrence of weak C–H···X (X = O, Hal) hydrogen bonds in conducting and superconducting cation radical salts of BEDT-TTF has been shown[1] to deeply influence the subtle solid state arrangement of the donor molecules within the conducting slabs. Indeed, the CH_2-CH_2 end groups of the BEDT-TTF molecules are most often engaged in weak C–H···X interactions with counter ions as in $(BEDT\text{-}TTF)_2I_3$ or $(BEDT\text{-}TTF)_8(SiW_{12}O_{40})$[2] or with solvent molecules which fit in the anionic layer as in $(BEDT\text{-}TTF)_2[Cu(CF_3)_4](Solvent)$[3] or $(BEDT\text{-}TTF)_4[Re_6S_6Cl_8](Solvent)$.[4] Those weak interactions effectively affect and control the relative orientation of the organic donor molecules within the conducting stacks or slabs, and, as a consequence, the topology of the HOMO–HOMO overlap interactions, the nature of the band structure (and Fermi surface) and the transport properties (semi-conducting or metallic conductivity, superconductivity).

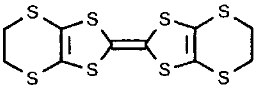
BEDT-TTF

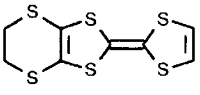
EDT-TTF

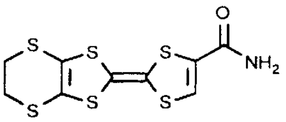
1

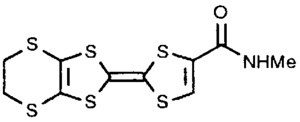
2

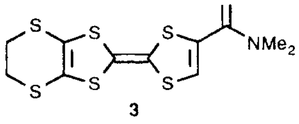
3

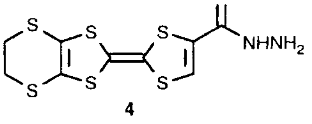
4

Tetrathiafulvalene-based molecules bearing functional groups with much *stronger* hydrogen bonding capabilities such as (i) alcohols, $Me_3TTF(CHMeOH)$,[5] $TTF(CH_2OH)_4$,[6] EDT-TTF-CH_2OH,[7] (ii) thioamides, (TTF-CSNHMe),[8] (iii) a uracil-derivatized TTF,[9] (iv) the anilinium phosphonate $PhNH_3^+Me_3TTF\text{-}PO_3H^-$ and its associated one-electron oxidation product, the neutral zwitterion, $[Me_3TTF\text{-}PO_3H^-]^{+\cdot}$, were recently described and engaged in cation radical salts.[10] Furthermore, the rigidity and dual hydrogen bond donor (N–H group) and hydrogen bond acceptor (oxygen atom of the carbonyl group) character of primary and secondary *amides* have been shown to drive the formation of well defined supramolecular arrays,[11] *via* N–H···O hydrogen bonds.[12,13] Elaborating upon those elements of predictability, the amide functionality has been actively engaged in molecular crystal chemistry and qualified as an efficient tool for the generation of extended hydrogen-bonded networks[14,15] as well as self-assembling supramolecular complexes.[16,17] Hence, the amide functionalization of the tetrathiafulvalene core is expected to offer a novel, rich crystal chemistry of both the neutral or oxidized form, through the competing requirements of hydrogen bonds, van der Waals and SOMO···SOMO overlap interactions.

In this paper, we describe the synthesis of such EDT-TTF functionalized amides, their electrochemical characterization and analyse their solid state structural organization. The presence of either primary or secondary amidic substituents, which both act as a hydrogen bond donor and hydrogen bond acceptor, is shown to compete in the solid state with primarily the S···S van der Waals interactions which stabilize the EDT-TTF dimer formation.

Synthesis

Several tetrathiafulvalenes substituted with amido groups have been prepared. In most cases, the flexible spacer between the TTF core and the functional group increases their solubility and facilitates their purification but provides extensive degrees of freedom to the molecules which become difficult to crystallize even in the neutral form. Such molecules have been already engaged in the preparation of Langmuir–Blodgett films, for example.[18] A TTF core derivatized with a shorter fragment, -SCH_2CONH_2, was also prepared by reacting the TTF thiolate with $BrCH_2CONH_2$.[19] The simplest primary amide, TTF-$CONH_2$,[20] was recently prepared by hydrolysis of the corresponding cyano derivative, TTF-CN, by analogy with the preparation of tetrakis(amido)tetrathiafulvalene from tetracyanotetrathiafulvalene.[21] The secondary amide

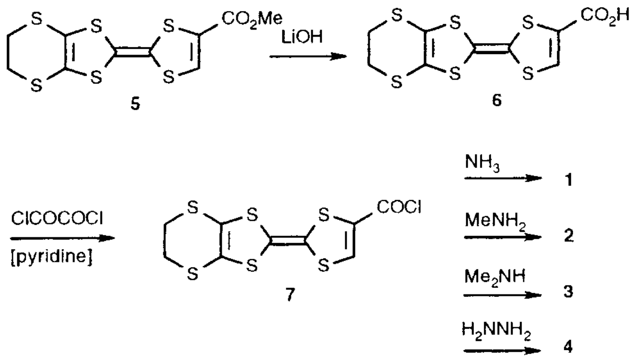

Scheme 1

TTF-CONHPh was prepared by reacting TTF-Li with phenyl isocyanate,[22,23] while the (*Z,E*) bifunctional analog was obtained several years ago from 3,3′(4′)-bis(chloroformyl)tetrathiafulvalene and aniline.[24] The disubstituted 3,4-bis(methylamido)tetrathiafulvalene has been prepared directly from the corresponding diester.[25] The tertiary amide, TTF-CONMe$_2$, was synthesized by the reaction of the acid chloride, TTF-COCl with dimethylamine,[25] as described earlier for the preparation of the (*Z,E*) bifunctional analog.[26]

As shown in Scheme 1, the three amides **1–3** and the hydrazide **4** were prepared from the corresponding ester **5** whose synthesis has been described elsewhere.[27] Hydrolysis to the carboxylic acid **6** was performed with LiOH as described by Kilburn.[28] Soxhlet extraction with acetone and recrystallization from this solvent afforded **6** as dark red crystals in 90% yield. Attempts to convert the ester **5** or the acid **6** directly to the desired amides were unsuccessful. Therefore, **6** was converted to the acid chloride **7** with oxalyl chloride and a catalytic amount of pyridine in 94% yield. Reaction of **7** with NH$_3$, MeNH$_2$, Me$_2$NH and H$_2$N-NH$_2$ afforded the corresponding amides **1–3** and the hydrazide **4**, respectively, in good yields. The three amides were recrystallized and their crystal structures determined by single crystal X-ray diffraction (see below).

Cyclic voltammetry experiments were performed in order to evaluate the oxidation potentials of those new donor molecules and the influence of a single amido group on the redox properties of the EDT-TTF core. As shown in Table 1, all four amide- or hydrazide-functionalized donors oxidize reversibly at about the same potential. Compared with that of EDT-TTF, the first oxidation potential is anodically shifted by 60–80 mV, confirming the electron-withdrawing effect of the amido group. Note, however, that this oxidation potential is still lower than that of BEDT-TTF. As a consequence, we expect cation radical salts of those donor molecules to form readily upon electrochemical oxidation and to crystallize into air-stable crystals.[29] The ambivalent character of the amido group, which exhibits both hydrogen bond donor and acceptor capabilities, is reflected by its ability to induce specific hydrogen bond networks in the solid state. The latter were identified and classified some years ago,[11,13,30] and are exemplified further in the crystal chemistry of the neutral forms **1–4** described below.

Table 1 Oxidation potentials of the amides **1–3** and the hydrazide **4** and some reference compounds. In V *vs.* SCE, *n*-Bu$_4$NPF$_6$ 0.05 M in CH$_3$CN at 100 mV s^{-1}, at 20 °C

	$E_{1/2}{}^1$	$E_{1/2}{}^2$
EDT-TTF	0.44	0.75
BEDT-TTF	0.56	0.80
EDT-TTF-CONH$_2$ **1**	0.49	0.81
EDT-TTF-CONHMe **2**	0.50	0.82
EDT-TTF-CONMe$_2$ **3**	0.47	0.80
EDT-TTF-CONHNH$_2$ **4**	0.48	0.88

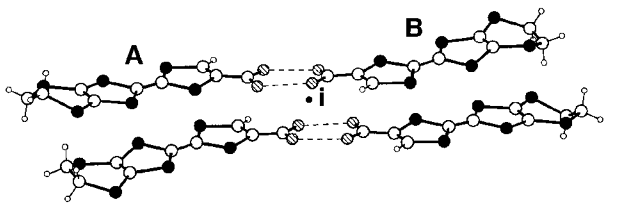

Fig. 1 Inversion-related dimers of hydrogen-bonded pairs of EDT-TTF-CO$_2$H in **6**.

Solid state structures: hydrogen bonding and van der Waals interactions

The crystal chemistry of the acid EDT-TTF-CO$_2$H, 6, and the primary amide EDT-TTF-CONH$_2$, 1

Crystal structures of the acid **6** and the three amides **1–3** were determined by single crystal X-ray diffraction. Details of crystallographic data, data collection and structure resolution are found in the Experimental section. The acid **6** crystallizes in the monoclinic system, space group *P*2$_1$/*n*. Two crystallographically independent molecules (A and B) are found in general positions in the unit cell. They are associated into AB pairs by two O–H···O hydrogen bonds (Fig. 1) to form the classical eight-membered cyclic motif, noted $R_2{}^2(8)$ in Etter's nomenclature,[31] with O···O distances of 2.58(2) and 2.60(2) Å, well in the expected range for carboxylic acids.[32] Two AB pairs are further associated through the inversion center into face-to-face dimers, a motif often encountered with such sulfur-rich molecules and stabilized by S···S van der Waals interactions, as observed in the structures of the neutral forms of EDT-TTF[33] or BEDT-TTF.[34] Indeed, the shortest S···S intermolecular contact within these pairs amounts to 3.66(3) Å, comparable to the sum of the van der Waals radii (3.60 Å).[35] As shown in Fig. 2, those pairs of dimers are further organized in the solid state in a herringbone pattern, with the ethylene end groups pointing toward the S atoms of a neighbouring EDT-TTF moiety. This structure is reminiscent of those reported by

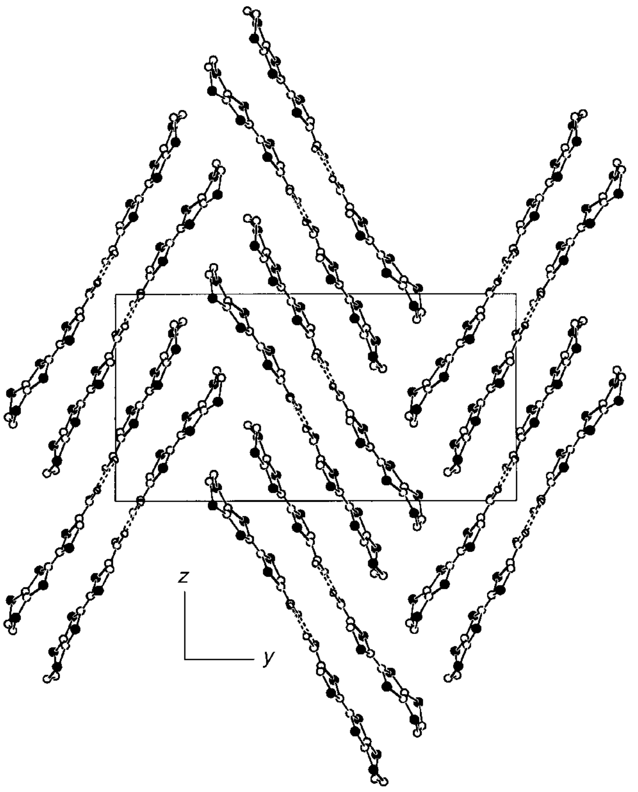

Fig. 2 Structure of EDT-TTF-CO$_2$H (**6**) projected along [100].

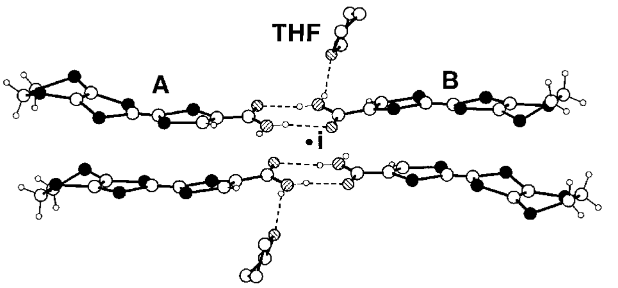

Fig. 3 The complex hydrogen bond network in (EDT-TTF-CONH$_2$)·(THF)$_{0.75}$, showing the inversion-related dimers of hydrogen-bonded pairs together with THF molecules.

Desiraju in carboxylic acid heterodimers where two stacked heterodimers are similarly related by an inversion centre while the lateral interactions are identified as originating from C–H···O hydrogen bonds.[36,37]

Interestingly, the primary amide **1** exhibits a very similar structural arrangement, the main difference arising from the presence of solvent molecules (THF), with one THF molecule in a general position and one THF molecule disordered on an inversion centre. Indeed, as shown in Fig. 3, two crystallographically independent molecules (A and B) are held together across two N–H$_s$···O hydrogen bonds involving the synplanar H atoms and form the prototypical $R_2^2(8)$ eight-membered cyclic motif.[31] Two pairs are further related by the inversion center to form face-to-face dimers, as observed in **6**, while the shortest S···S distance within this A–B pair amounts to 3.561 Å. The main difference with the structure of the acid **6** now arises from the effect of the additional antiplanar H$_a$ hydrogen atoms of the primary amide **1**. Within the dimer, two such H$_a$ hydrogen atoms are engaged in N–H$_a$···O bonds with the carbonyl oxygen atoms of the neighbouring molecule while two others are engaged in an N–H$_a$···O bond with the oxygen atom of a THF molecule. As shown in Fig. 4, the whole structure of **1** appears then as an expansion of the structure of the acid **6**, made necessary by the presence of the extra antiplanar H$_a$ hydrogen atom of the primary amide. The structural characteristics of those hydrogen bonds are given in Table 2. Bond distances and angles are in the expected range for N–H···O hydrogen bonds.[38] Note the C=O···H angle (ϕ) values close to 120° for the two synplanar H$_s$ atoms while the antiplanar H$_a$ exhibits a more linear conformation.[39]

In the latter two structures, one has observed the complementary effect of two different intermolecular interactions, the hydrogen bonding requirements of the acid and primary amide groups which lead to the $R_2^2(8)$ motif and the van der Waals S···S interactions which stabilize the face-to-face arrangement of the EDT-TTF moieties. The latter dispersion forces exercise a strong control over the structural arrangement since they shift the inversion center in between the two pairs while it is normally found at the center of the $R_2^2(8)$ motif in homodimers. On the other hand, the hydrogen bond patterns adopted by both the acid and the primary amide are those expected for such systems, albeit the more severe constraints which aim at satisfying both N–H$_a$···O and N–H$_s$···O hydrogen bonds in the primary amide are reflected by slightly more distorted geometries and the incorporation of THF solvate molecules.

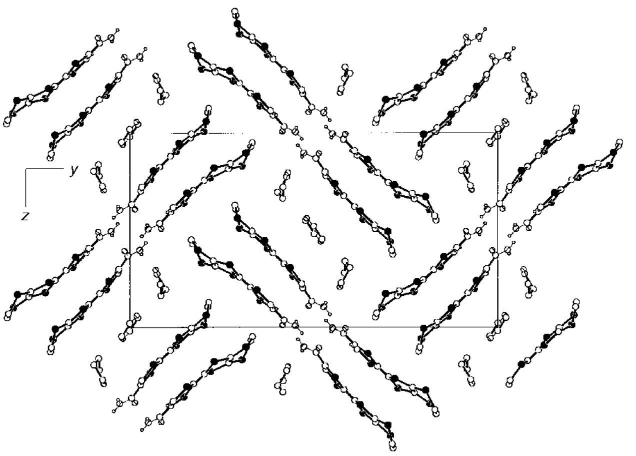

Fig. 4 Structure of (EDT-TTF-CONH$_2$)·(THF)$_{0.75}$ projected along [100]. The THF molecule in general position is hydrogen-bonded to **1** while an additional THF molecule is disordered on the inversion centre.

The secondary amide EDT-TTF-CONHMe, 2

Compound **2** crystallizes in the orthorhombic system, space group $P2_12_12_1$ with two crystallographically independent molecules in the asymmetric unit (denoted by A and B in the following). In both molecules, the amidic group adopts a *trans* configuration with the H atom in the antiplanar position. Short N–H···O hydrogen bonds (Table 3) are found between alternating A and B molecules along the [010] twofold screw axis, which give rise to a characteristic C(4) chain motif (Fig. 5). Of particular note here are the short C–H···O interactions identified in this structure between the H atom located *ortho* to the amidic group and the O atom of the carbonyl. As shown in Table 4, their structural characteristics are indeed very close to those observed with the amidic hydrogen atoms and these C–H···O interactions can thus be qualified as C–H···O *hydrogen bonds*, which adopt here a C(5) motif along the [010] twofold screw axis. The second order combination of those two motifs, C(4) and C(5), gives rise to the novel cyclic motif, noted $R_2^1(7)$ in Fig. 6. Such an activation of the *ortho* hydrogen atom to afford C(sp^2)–H···O hydrogen bonds[40] has been observed in the crystal packing of quinones,[41] α,β-unsaturated[42] or aromatic[43,44] carboxylic acids, dicyanobenzene,[45] and very recently cubane-carboxylic acids.[46] They have been shown to play a major role in stabilizing crystal structures[46,47] and were identified earlier in

Table 2 Hydrogen bond characteristics in EDT-TTF-CONH$_2$, **1** (Indices A and B refer to molecules A and B, respectively; indices a and s refer to the antiplanar and synplanar configurations of the amidic hydrogen atoms, respectively)

	D···A dist.	H···A dist.	α/°	ϕ/°	Motif
N$_A$–H$_{As}$···O$_B$	3.02(2)	2.18(2)	164.9(7)	124(1)	$R_2^2(8)$
N$_A$–H$_{Aa}$···O$_B$	3.04(2)	2.26(2)	150.7(6)	154(2)	D
N$_B$–H$_{Bs}$···O$_A$	2.83(2)	1.99(2)	168.4(8)	119(1)	$R_2^2(8)$
N$_B$–H$_{Ba}$···O(THF)	2.90(2)	2.14(2)	146.0(8)	—	D

Table 3 Hydrogen bond characteristics in EDT-TTF-CONHMe **2** (Indices A and B refer to molecules A and B, respectively; index a refers to the antiplanar configuration of the amidic hydrogen atom)

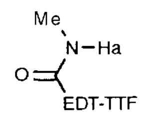

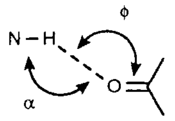

	D···A dist.	H···A dist.	α/°	ϕ/°	Motif
N_A–$H_{Aa}\cdots O_B$	2.949(5)	2.102(5)	168.1(1)	130.4(3)	C(4)
N_B–$H_{Ba}\cdots O_A$	2.952(5)	2.119(5)	162.7(1)	138.3(2)	C(4)
C_A–$H_A\cdots O_B$	3.324(5)	2.421(5)	163.8(1)	122.0(2)	C(5)
C_B–$H_B\cdots O_A$	3.126(6)	2.217(6)	165.3(1)	140.0(3)	C(5)

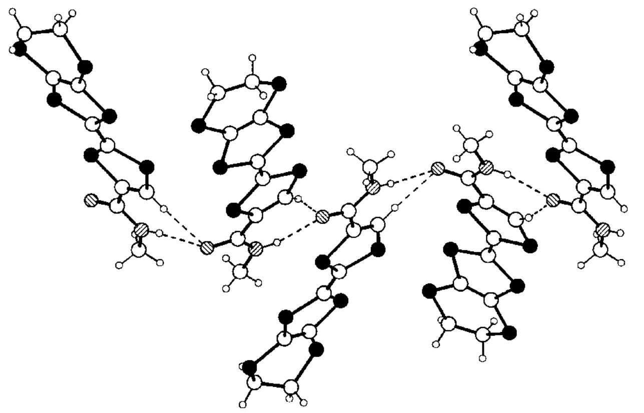

Fig. 5 The hydrogen-bonded chain of EDT-TTF-CONHMe (**2**) molecules combining the C4 N–H···O and the C5 C–H···O motifs.

the TTF·*p*-chloranil charge-transfer complex where they become collectively activated upon charge-transfer along the neutral-to-ionic transition.[48] A preliminary CSD search on simple conjugated methylamides confirmed the occurrence of this C–$H_{ortho}\cdots$O hydrogen bond, observed for example in *N*-methylbenzamide[13] (H···O: 2.482 Å, $\alpha = 146.4°$) or *N*-methylnicotinamide[49] (H···O: 2.402 Å, $\alpha = 136.1°$) where it gives rise in both structures to this characteristic $R_2^1(7)$ chelating ring. Of particular note in this structure is the absence of face-to-face EDT-TTF–EDT-TTF dimers, a recurrent motif observed in the unsubstituted molecule as well as in **1**, **3** and **6**. Clearly here, the structural requirements of the N–H···O and C–H···O hydrogen bonds took over the EDT-TTF–EDT-TTF dimer formation. Indeed, besides one single intermolecular short S···S distance at 3.407 Å, all other S···S distances are larger than 3.697 Å.

The tertiary amide EDT-TTF-CONMe$_2$ 3

The tertiary amide **3** lacks any of the strong OH or NH hydrogen bond donors found in **1** or **2**. It crystallizes in the orthorhombic system, space group $P2_12_12_1$, with one molecule in general position in the unit cell. A herringbone pattern is observed here (Fig. 7), reminiscent of that described above for the acid **6**, with the outer ethylenic groups pointing towards the sulfur atoms of a neighbouring EDT-TTF moiety. The shortest S···S van der Waals contact amounts to 3.655(3) Å.

Molecular structure analysis

The four structures described above offer a unique opportunity to compare the geometrical characteristics of the donor molecules, each of them functionalized with a different electron-withdrawing group. The salient intramolecular bond lengths and angles, and torsion angles (along the S–S axis) of the two dithiole rings are collected in Table 4, together with reference data for the unsubstituted EDT-TTF. Neutral, non-oxidized tetrathiafulvalenes are well known to easily distort by torsion of the dithiole rings along the S–S axis. This folding, observed in EDT-TTF at 12 and 17° respectively for the β_1 and β_2 values (Table 4), is strongly lowered in the 1,3-dithiole ring substituted with the carboxylic or amidic group in **1–3** and **6,** the strongest effect being mainly observed in the acid **6** and the primary amide **1**. This observation, together with the lengthening of the C=C bond (noted b in Table 4) and concomitant shortening of the S–C bond (noted c in Table 4) upon functionalization, confirms the sizeable contribution of the mesomeric forms **1′–3′** in the electronic structure of **1–3** (as also in **6**) already observed and analyzed by Bryce and co-workers in similar TTF derivatives.[25]

Experimental

4,5-Ethylenedithio-4′-carboxytetrathiafulvalene 6

A solution of LiOH·H_2O (1.8 g, 42.9 mmol in 30 ml H_2O) was added to a stirred solution of EDT-TTF-CO_2Me **5** (3 g, 8.5 mmol) in 1,4-dioxane (200 mL) at room temperature. After stirring for 15 h, HCl 5 M (8.5 mL, 42.8 mmol) was added dropwise and the solution stirred for 10 min. Diethyl ether (200 mL) and water (50 mL) were added followed by HCl 5 M until the pH of the water phase reached 1–2. The organic layer was decanted, dried over $MgSO_4$ and evaporated under reduced pressure. The red solid was Soxhlet extracted with acetone to afford **6** as red crystals (2.6 g, 90%), mp 216–217 °C (decomp.) (Analysis found: C, 31.88; H, 1.83; S, 55.08; $C_9H_6O_2S_6$ requires: C, 31.93; H, 1.79; S, 56.83%); ν_{max}/cm^{-1} (KBr) 3050–2250 (OH), 1651 (CO); λ_{max}/nm (ε/dm^3 mol^{-1} cm^{-1}) (THF) 415 (2.1 10^3); δ_H(200 MHz, d_6-DMSO) 7.70 (s, 1H, C=CH), 3.38 (s, 4H, CH_2-CH_2); δ_C(50 MHz, DMSO) 160.09 (CO_2H), 132.70 (=CH), 128.77, 112.74, 103.57, 104.80 (C=C) and 29.45 (CH_2-CH_2); *m*/*z* 338 (M^+, 85%), 294 (M^+-CO_2, 33%), 266 ($M^+-CO_2-CH_2CH_2$, 33%).

4,5-Ethylenedithiotetrathiafulvalene-4′-carbonyl chloride 7

Oxalyl chloride (0.4 mL, 4.62 mmol) and pyridine (1 μL) were added to a stirred THF solution (60 mL) of the acid **6** (0.55 g, 1.5 mmol) under nitrogen at 45 °C. The mixture was stirred for 3 h and filtered, the volume was reduced to 10 mL and the product precipitated by addition of dry hexane to afford the acid chloride **7** as a purple microcrystalline powder (0.55 g, 94%), mp 165–168 °C (decomp.) (Analysis found: C, 30.65; H, 1.41; S, 51.73; Cl, 10.17. $C_9H_5OS_6Cl$ requires: C, 30.28; H, 1.41; S, 53.89; Cl, 9.93%); ν/cm^{-1} (KBr) 1710 (CO); δ_H(200 MHz, $CDCl_3$) 7.78 (s, 1H, C=CH), 3.31 (s, 4H, CH_2-CH_2); δ_C(50 MHz, $CDCl_3$) 141.23 (=CH) and 30.17 (CH_2-CH_2); *m*/*z* 356 (M^+, 85%), 328 (M^+-CH_2-CH_2, 72%).

Table 4 Selected geometrical characteristics of **1**, **2**, **3** and **6**

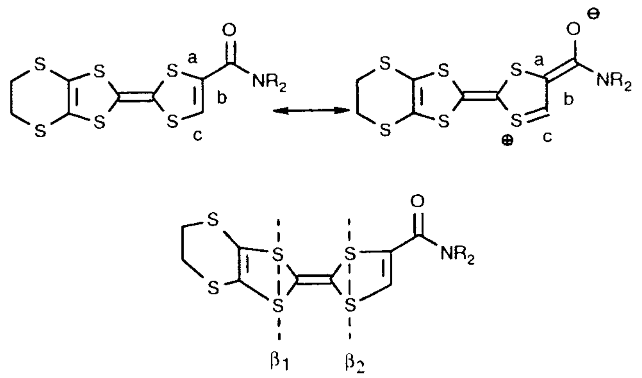

	Tors. angle β_1	Tors. angle β_2	C–S dist. a	C=C dist. b	C–S dist. c
6 A	9.6(6)	3.5(6)	1.75(2)	1.36(2)	1.71(2)
B	7.8(5)	1.4(6)	1.75(2)	1.32(2)	1.66(2)
1 A	23.0(3)	2.6(3)	1.742(8)	1.335(10)	1.701(7)
B	8.0(4)	4.6(3)	1.754(8)	1.325(10)	1.719(7)
2 A	1.4(4)	6.7(3)	1.746(4)	1.316(6)	1.714(5)
B	8.2(4)	6.9(3)	1.757(5)	1.328(6)	1.720(5)
3	3.4(8)	3.0(7)	1.760(7)	1.31(1)	1.746(8)
EDT-TTF	17	12	1.745(4)	1.317(6)	1.745(4)

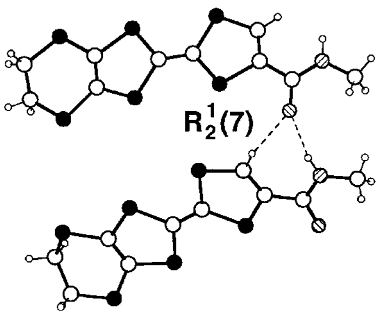

Fig. 6 A detail of the R$_2{}^1$(7) chelate ring in (**2**) which results from the second order association of the two primary motifs, C4 and C5.

4,5-Ethylenedithio-4′-carbamoyltetrathiafulvalene 1

A solution of the acid choride **7** (150 mg, 0.42 mmol) in dry THF (10 mL) is added dropwise to an NH_3 saturated THF solution (10 mL). The solution turned yellow and was stirred for 1 h, filtered, and concentrated to afford **1** as red needles after recrystallization from THF (130 mg, 92%), mp 214–215 °C (decomp.) (Analysis found: C, 33.17; H, 2.72; N, 3.71; S, 52.56. $C_9H_7ONS_6{\cdot}THF_{0.75}$ requires: C, 33.78; H, 2.55; N, 3.94; S, 56.83%); ν/cm^{-1} (KBr) 3417–3173 (NH_2), 1647 (C=O); λ_{max}/nm (ε/dm^3 mol^{-1} cm^{-1}) (THF) 395 (1.9 10^3); δ_H(200 MHz, d_6-DMSO) 7.95 (s, 1H, NH_2), 7.55 (s, 1H, C=CH), 3.38 (s, 4H, CH_2-CH_2); δ_C(50 MHz, d_6-DMSO) 160.35 (C=O), 134.25 (C-CO), 125.04 (=CH), 103.38–113.02 (C=C) and 29.47 (CH_2-CH_2); *m*/*z* 337 (M$^+$, 100%), 309 (M$^+$−CH_2-CH_2, 84%).

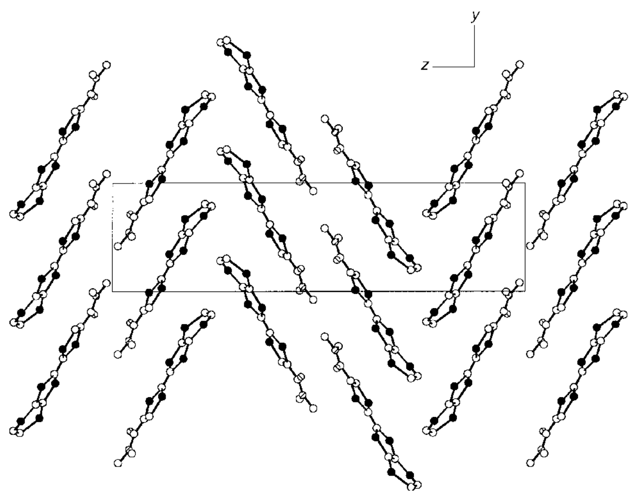

Fig. 7 Structure of EDT-TTF-CONMe$_2$ (**3**) projected along [100].

4,5-Ethylenedithio-4′-(methylcarbamoyl)tetrathiafulvalene 2

To a 2 M THF solution of methylamine (5.3 mL, 10.65 mmol) was added dropwise the acid chloride **7** (250 mg, 0.71 mmol) dissolved in dry THF (5 mL). After stirring for 1 h, the solution was concentrated and extracted with CH_2Cl_2. The organic layer was dried over $MgSO_4$ and evaporated to afford **2** as orange crystals after recrystallization from CH_3CN (190 mg, 77%), mp 216–217 °C (Analysis found: C, 34.21; H, 2.76; N, 3.92; S, 54.64. $C_{10}H_9ONS_6$ requires C, 34.16; H, 2.58; N, 3.98; S, 53.89%); ν/cm^{-1} (KBr) 3336–3275 (NH), 1614 (C=O), 1572 (NH); λ_{max}/nm (ε/dm^3 mol^{-1} cm^{-1}) (THF) 380 sh; δ_H(200 MHz, d_6-DMSO) 8.42 (q, 1H, NH, ^3J(H–H) = 4.5 Hz), 7.44 (s, 1H, C=CH), 3.38 (s, 4H, CH_2-CH_2), 2.66 (d, 3H, CH_3, ^3J(H–H) = 4.5 Hz); δ_C(50 MHz, DMSO) 159.17 (C=O), 133.65 (C-CO), 124.22 (=CH), 112.8–113.15 (C=C), 29.60 (CH_2-CH_2) and 26.10 (CH_3); *m*/*z* 351 (M$^+$, 100%), 323 (M$^+$−CH_2-CH_2, 65%).

4,5-Ethylenedithio-4′-(*N*,*N*-dimethylcarbamoyl) tetrathiafulvalene 3

To a 2 M THF solution of dimethylamine (1.75 mL, 3.5 mmol) diluted in dry THF (10 mL) was added dropwise the acid chloride **7** (250 mg, 0.71 mmol) dissolved in dry THF (10 mL). After stirring for 1 h, the solution was filtered and evaporated. The orange solid was recrystallized in CH_3CN to afford **3** as orange crystals (180 mg, 70%), mp 177–178 °C (Analysis found: C, 36.33; H, 3.17; N, 3.68; S, 52.78. $C_{11}H_{11}ONS_6$ requires: C, 36.14; H, 3.03; N, 3.83; S, 52.62%); ν/cm^{-1} (KBr) 1597 (C=O); λ_{max}/nm (ε/dm^3 mol^{-1} cm^{-1}) (THF) 380 sh; δ_H(200 MHz, $CDCl_3$) 6.60 (s, 1H, C=CH), 3.29 (s, 4H, CH_2-CH_2), 3.07 (s, 6H, CH_3); *m*/*z* 365 (M$^+$, 100%), 337 (M$^+$−CH_2-CH_2, 56%).

Table 5 X-Ray structure determination data

Crystal data	**6**	**1**·(THF)$_{0.75}$	**2**	**3**
Emp. formula	$C_9H_6O_6S_6$	$C_{12}H_{13}NO_{1.75}S_6$	$C_{10}H_9NOS_6$	$C_{11}H_{11}NOS_6$
Formula weight	338.50	391.59	351.54	365.57
Temperature/K	180(2)	180(2)	293(2)	293(2)
Crystal system	Monoclinic	Monoclinic	Orthorhombic	Orthorhombic
Space group	$P2_1/n$	$P2_1/n$	$P2_12_12_1$	$P2_12_12_1$
Unit cell dim.				
a/Å	6.3720(8)	6.3477(6)	7.6636(15)	6.2990(13)
b/Å	27.142(6)	30.765(3)	17.584(4)	7.886(2)
c/Å	14.238(2)	16.438(2)	21.553(4)	29.631(6)
α/°	90	90	90	90
β/°	92.29(2)	95.681(11)	90	90
γ/°	90	90	90	90
Volume/Å^3	2460.5(7)	3194.4(5)	2904.5(10)	1471.9(5)
Z	8	8	8	4
Density (calcd.)/g cm^{-3}	1.828	1.628	1.608	1.650
Abs. coeff./mm^{-1}	1.09	0.855	0.927	0.918
F(000)	1376	1616	1440	752
Refls. collected	19288	23683	13914	3802
Independent refls.	4613	6153	4459	2845
R_{int}	0.44	0.22	0.0476	0.072
$R(F)[I > 2\sigma(I)]$	0.082	0.069	0.036	0.047
$wR(F^2)$	0.19	0.151	0.071	0.20

4,5-Ethylenedithio-4′-carbazoyltetrathiafulvalene 4

A solution of the acid chloride **7** (250 mg, 0.7 mmol) in 20 mL of dry THF was added dropwise to a 1 M THF solution of hydrazine (7 mL, 7 mmol). The mixture was stirred for 1 h, filtered and evaporated. The orange solid was recrystallized from acetone to afford **4** as orange microcrystals (180 mg, 73%), mp 194–195 °C (Analysis found: C, 30.59; H, 2.58; N, 7.81; S, 51.61. $C_9H_8ON_2S_6$ requires: C, 30.66; H, 2.29; N, 7.95; S, 54.57%); ν/cm^{-1} (KBr) 1664 (C=O); δ_H(200 MHz, d_6-DMSO) 7.42 (s, 1H, =CH), 3.37 (s, 4H, CH_2-CH_2); m/z 352 (M^+, 100%), 324 ($M^+ - CH_2$-CH_2, 68%).

X-Ray structure determinations†

The data collections were performed on a Stoe IPDS system for **1**, **2** and **6**, and on an Enraf-Nonius Mach 3 diffractometer for **3**. The Siemens SHELXTL package was used for the solution and refinements of the X-ray structures. No absorption correction was applied. In **1**, **2** and **3**, hydrogen atoms were introduced at calculated positions and not refined (riding model). Furthermore, in the primary amide **1**, one C atom of the ethylenic group was disordered on two positions (C17A, C17B). Similarly, every C atom of the ethylenic groups of the two crystallographically independent molecules in **2** was found disordered on two positions as well as one S atom linked to the ethylenic group. The C atoms of the ethylenic group in **3** were also disordered on two positions. Those disordered atoms were all refined isotropically. Despite low temperature data collections for the acid **6**, the number of strong reflections is not as large when compared with the total number of independent reflections, indicating a somewhat poor crystal quality. Accordingly, only S atoms were refined anisotropically while C and O atoms were refined isotropically and hydrogen atoms introduced at calculated positions and not refined (riding model). The acidic hydrogen atom in **6** could not be identified in the Fourier difference map and was not introduced. Crystal data and details of data collection and structure refinement are given in Table 5.

Acknowledgements

Financial support (to K. H.) from the MENRT is gratefully acknowledged. This work was also supported by the CNRS, the University of Nantes and the Région Pays de la Loire.

References

1 M.-H. Whangbo, J. M. Williams, A. J. Schultz, T. J. Emge and M. A. Beno, *J. Am. Chem. Soc.*, 1987, **109**, 90; M.-H. Whangbo, D. Jung, J. Ren, M. Evain, J. J. Novoa, F. Mota, S. Alvarez, J. M. Williams, M. A. Beno, A. M. Kini, H. H. Wang and J. R. Ferraro, in *The Physics and Chemistry of Organic Superconductors*, eds. C. Saito and S. Kagoshima, Springer Verlag, Berlin, Heidelberg, 1990, p. 262.

2 A. Davidson, K. Boubekeur, A. Pénicaud, P. Auban, C. Lenoir, P. Batail and G. Hervé, *J. Chem. Soc., Chem. Commun.*, 1989, 1373.

3 J. A. Schlueter, J. M. Williams, U. Geiser, J. D. Dudek, M. E. Kelly, S. A. Sirchio, K. D. Carlson, D. Naumann, T. Ray and C. F. Campana, *Adv. Mater.*, 1995, **7**, 634.

4 A. Pénicaud, K. Boubekeur, P. Batail, E. Canadell, P. Auban-Senzier and D. Jérome, *J. Am. Chem. Soc.*, 1993, **115**, 4101.

5 A. Dolbecq, M. Fourmigué, P. Batail and C. Coulon, *Chem. Mater.*, 1994, **6**, 1413.

6 A. Dolbecq, A. Guirauden, M. Fourmigué, K. Boubekeur, P. Batail, M.-M. Rohmer, M. Bénard, C. Coulon, M. Sallé and P. Blanchard, *J. Chem. Soc., Dalton Trans.*, 1999, 1241.

7 P. Blanchard, K. Boubekeur, M. Sallé, G. Duguay, M. Jubault, A. Gorgues, J. D. Martin, E. Canadell, P. Auban-Senzier, D. Jérome and P. Batail, *Adv. Mater.*, 1992, **4**, 579.

8 A. J. Moore, M. R. Bryce, A. S. Batsanov, J. N. Heaton, C. W. Lehmann, J. A. K. Howard, N. Robertson, A. E. Underhill and I. F. Perepichka, *J. Mater. Chem.*, 1998, **8**, 1541.

9 O. Neilands, S. Belyakov, V. Tilika and A. Edzina, *J. Chem. Soc., Chem. Commun.*, 1995, 325.

10 A. Dolbecq, M. Fourmigué, F. C. Krebs, P. Batail, E. Canadell, R. Clérac and C. Coulon, *Chem. Eur. J.*, 1996, **2**, 1275.

11 J. Bernstein, M. C. Etter and L. Leiserowitz, in *Structure Correlation*, eds. H.-B. Bürgi and J. D. Dunitz, vol. 2, VCH, Weinheim, 1994, ch. 11.

12 L. Leiserowitz and G. M. J. Schmidt, *J. Chem. Soc. (A)*, 1969, 2372.

13 L. Leiserowitz and M. Tuval, *Acta Crystallogr., Sect. B*, 1978, **34**, 1230.

14 V. A. Russel and M. D. Ward, *Chem Mater.*, 1996, **8**, 1654.

15 S. Palacin, D. N. Chin, E. E. Simanek, J. C. MacDonald, G. M. Whitesides, M. T. McBride and G. T. R. Palmore, *J. Am. Chem. Soc.*, 1997, **119**, 11 807.

16 D. S. Lawrence, T. Liang and M. Levett, *Chem. Rev.*, 1995, **95**, 2229.

---

†CCDC reference number 1145/174. See http://www.rsc.org/suppdata/jm/1999/2373 for crystallographic files in .cif format.

17 R. A. Pascal, J. Spergel and D. Van Engen, *Tetrahedron Lett.*, 1986, **27**, 4099; P. D. Beer, D. Hesek, J. Hofacova and S. E. Stockes, *J. Chem. Soc., Chem. Commun.*, 1992, 270.
18 R. P. Parg, J. D. Kilburn, M. C. Petty, C. Pearson and T. G. Ryan, *Synthesis*, 1994, 613.
19 G. Ono, A. Izuoka, T. Sugawara and Y. Sugawara, *J. Mater. Chem.*, 1998, **8**, 1703.
20 G. Cooke, A. K. Powell and S. L. Health, *Synthesis*, 1995, 1411.
21 S. Yoneda, T. Kawase, M. Inaba and Z. Yoshida, *J. Org. Chem.*, 1978, **43**, 595.
22 A. S. Batsanov, M. R. Bryce, G. Cooke, A. S. Dhindsa, J. N. Heaton, J. A. K. Howard, A. J. Moore and M. C. Petty, *Chem. Mater.*, 1994, **6**, 1419.
23 A. J. Moore, M. R. Bryce, A. S. Batsanov, J. C. Cole and J. A. K. Howard, *Synthesis*, 1995, 675.
24 C. U. Pittman, Jr. , M. Narita and Y. F. Liang, *J. Org. Chem.*, 1976, **41**, 2855.
25 A. S. Batsanov, M. R. Bryce, J. N. Heaton, A. J. Moore, P. J. Skabara, J. A. K. Howard, E. Orti, P. M. Viruela and R. Viruela, *J. Mater. Chem.*, 1995, **5**, 1689.
26 S. Yoneda, T. Kawase, Y. Yasuda and Z. Yoshida, *J. Org. Chem.*, 1979, **44**, 1728.
27 P. Blanchard, M. Sallé, G. Duguay, M. Jubault and A. Gorgues, *Tetrahedron Lett.*, 1992, **33**, 2685.
28 R. P. Parg, J. D. Kilburn, M. C. Petty, C. Pearson and T. G. Ryan, *J. Mater. Chem.*, 1995, **5**, 1609.
29 K. Heuzé, M. Fourmigué, P. Batail, E. Canadell and P. Auban-Senzier, *Chem. Eur. J.*, 1999, **5**, 2971.
30 S. Weinstein and L. Leiserowitz, *Acta Crystallogr., Sect. B*, 1980, **36**, 1406.
31 Within this nomenclature, $R_d^a(n)$ describes a cyclic motif made of one type of hydrogen bonds involving d hydrogen atoms, a hydrogen bond acceptors within a ring of n atoms (including H atoms) while C_n indicates an infinite chain-like motif of n atoms (including H atoms) in the repeat unit. See: M. Etter: *Acc. Chem. Res.*, 1990, **23**, 120.
32 L. Leiserowitz, *Acta Crystallogr., Sect. B*, 1976, **32**, 775.
33 B. Garreau, D. De Montauzon, P. Cassoux, J.-P. Legros, J.-M. Fabre, K. Daoud and S. Chakroune, *New J. Chem.*, 1995, **19**, 161.
34 H. Kobayashi, A. Kobayashi, Y. Sasaki, G. Saito and H. Inokuchi, *Bull. Chem. Soc. Jpn.*, 1986, **59**, 301; P. Guionneau, C. J. Kepert, D. Chasseau, M. R. Truer and P. Day, *Synth. Met.*, 1997, **86**, 1973.
35 A. Bondi, *J. Phys. Chem.*, 1964, **68**, 441.
36 R. Taylor and O. Kennard, *J. Am. Chem. Soc.*, 1982, **104**, 5063.
37 C. V. K. Sharma, K. Panneerselvam, T. Pilati and G. R. Desiraju, *J. Chem. Soc., Perkin Trans. 2*, 1993, 2209.
38 R. Taylor, O. Kennard and W. Versichel, *Acta Crystallogr., Sect. B*, 1984, **40**, 280.
39 R. Taylor, O. Kennard and W. Versichel, *J. Am. Chem. Soc.*, 1983, **105**, 5761.
40 G. R. Desiraju, *Angew. Chem., Int. Ed. Engl.*, 1995, **34**, 2311.
41 J. Bernstein, M. D. Cohen and L. Leiserowitz, in *The Chemistry of the Quinoid Compounds*, Part I, ed. S. Patai, Interscience, New York, 1974, p. 37.
42 L. Leiserowitz, *Acta Crystallogr., Sect. B*, 1976, **32**, 775.
43 M. G. Takwale and L. M. Pant, *Acta Crystallogr., Sect. B*, 1971, **27**, 1152.
44 M. Bailey and C. J. Brown, *Acta Crystallogr.*, 1967, **22**, 387.
45 H. Guth, G. Heger and U. Drück, *Z. Kristallogr.*, 1982, **159**, 185.
46 S. S. Kuduva, D. C. Craig, A. Nangia and G. R. Desiraju, *J. Am. Chem. Soc.*, 1999, **121**, 1936.
47 G. R. Desiraju, *Acc. Chem. Res.*, 1991, **24**, 290; T. Steiner, *Chem. Commun.*, 1997, 727.
48 P. Batail, S. J. LaPlaca, J. J. Mayerle and J. B. Torrance, *J. Am. Chem. Soc.*, 1981, **103**, 951.
49 T. Srikrishnan and R. Parthasarathy, *Acta Crystallogr., Sect. C*, 1990, **46**, 1723.

Paper 9/02852H